

Electromagnetic Structure of Few-Nucleon Systems: a Critical Review

R. Schiavilla ^a

^aJefferson Lab, Newport News, Virginia 23606

and

Department of Physics, Old Dominion University, Norfolk, Virginia 23529

Our current understanding of the structure of nuclei with $A \leq 8$, including energy spectra, electromagnetic form factors, and capture reactions, is critically reviewed within the context of a realistic approach to nuclear dynamics based on two- and three-nucleon interactions and associated electromagnetic currents.

1. Introduction

In the present talk I will review the simple, traditional picture of the nucleus as a system of point-like nucleons interacting among themselves via effective many-body potentials, and with external electro-weak probes via effective many-body currents. I will also discuss the extent to which this picture, the so called “nuclear standard model”, is successful in predicting a number of nuclear properties for systems with mass number $A \leq 8$, including energy spectra of low-lying states, electromagnetic form factors, and low-energy capture reactions.

2. Interactions and Energy Spectra

The Hamiltonian in the nuclear standard model is taken to consist of a non-relativistic kinetic energy operator, and two- and three-nucleon potentials. The two-nucleon potential consists of a long range part due to pion exchange, and a short-range part parameterized either in terms of heavy meson exchanges as, for example, in the Bonn potential [1], or via suitable operators and strength functions, as in the Argonne v_{18} (AV18) potential [2]. The short-range terms in these potentials are then constrained to fit pp and np scattering data up to energies of $\simeq 350$ MeV in the laboratory, and the deuteron binding energy. The modern models mentioned above include isospin-symmetry-breaking components, and provide fits to the Nijmegen data-base [3] characterized by χ^2 per datum close to one. They should therefore be viewed as phase-equivalent.

A major difference among these modern potential models, however, is in the treatment of non-localities, particularly those associated with off-the-energy-shell prescriptions of the one-pion-exchange (OPE) term. The AV18 as well as the Nijmegen models incorporate the on-shell form of the OPE term, which leads to a local tensor component. The Bonn potential, on the other hand, includes the off-shell extension predicted by pseudo-scalar coupling of pions to nucleons, and hence has a strongly non-local tensor component. More

than two decades ago, Friar and collaborators [4] showed that different OPE off-shell extensions can be related to each other via a unitary transformation, and that differences in predictions for observables sensitive to OPE, such as the triton binding energy or the deuteron tensor polarization at moderate momentum transfers ($\leq 5 \text{ fm}^{-1}$), can be, to a large extent, removed by performing *consistent* calculations, namely calculations using three-nucleon interactions and charge operators that obey the unitary equivalence of the OPE interaction. An example of this type of calculations is illustrated in Fig. 1, where the deuteron tensor polarizations corresponding to the Bonn potential and to the AV18 deuteron wave function and charge operator, unitarily transformed to match the off-shell extension of the Bonn OPE, are compared. The remaining differences at the larger values of momentum transfer are presumably originating from additional short-range non-localities present in the Bonn model. It should be stressed that *consistent* calculations of the type alluded to above have been carried out up until now only for the deuteron. It would be interesting to verify these expectations also for the case of other observables, such as the triton binding energy, for example.

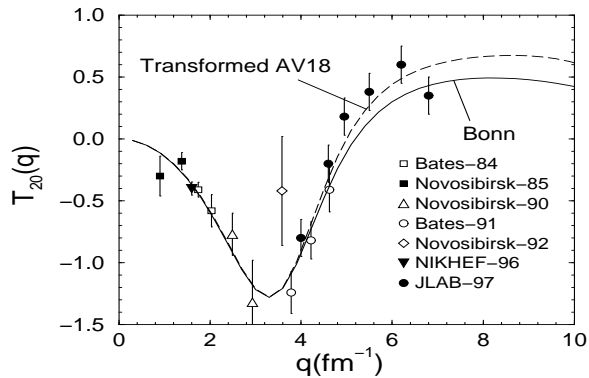


Figure 1. The deuteron tensor polarizations obtained with Bonn potential and “unitarily transformed” AV18 deuteron wave function and charge operators.

It is now well established that two-nucleon potentials alone underbind nuclei [5,6]: for example, the AV18 and Bonn models give [6], in numerically exact calculations, binding energies of 24.28 MeV and 26.26 MeV respectively, which should be compared to the experimental value of 28.3 MeV. Moreover, it has been shown in Ref. [5] that, for example, ^6Li and ^7Li are unstable against breakup into αd and αt clusters, respectively, and that energy differences are not, in general, well predicted, when only two-nucleon potentials are retained in the Hamiltonian.

Important components of the three-nucleon potential are due to the internal structure of the nucleon. Since all degrees of freedom other than the nucleon have been integrated out, the presence of virtual Δ resonances, for example, induces three-nucleon potentials. Current three-nucleon potential models are reviewed by Carlson [7] in these proceedings. These newly developed models include the “long-range” term, resulting from the interme-

diate excitation of a Δ with pion exchanges involving the other two nucleons, known as the Fujita-Miyazawa term [8], as well as multipion exchange terms involving excitation of one or two Δ 's, so-called pion-ring diagrams, and the terms arising from S-wave pion rescattering, required by chiral symmetry. There are four strength parameters which are then determined by fitting the energies of $\simeq 20$ low-lying states of systems with $A \leq 8$ nuclei in exact Green's function Monte Carlo calculations. The resulting energy spectra for these systems are in good agreement with the experimental ones [7]. In particular, the underbinding of neutron-rich nuclei, such as ^6He and ^8Li , which had proven to be a problem with earlier models of three-nucleon potentials, is resolved to a large extent.

3. Electromagnetic Current and Form Factors

The nuclear current operator consists of one- and many-body terms that operate on the nucleon degrees of freedom. The one-body operator has the standard expression in terms of single-nucleon convection and magnetization currents. The two-body current operator has “model-independent” and “model-dependent” components (for a review, see Ref. [9]). The model-independent terms are obtained from the two-nucleon potential, and by construction satisfy current conservation with it. The leading operator is the isovector “ π -like” current obtained from the isospin-dependent spin-spin and tensor interactions. The latter also generate an isovector “ ρ -like” current, while additional model-independent isoscalar and isovector currents arise from the central and momentum-dependent interactions. These currents are short-ranged and numerically far less important than the π -like current. Finally, models for three-body currents have been derived in Ref. [10], by gauging the two-pion exchange three-nucleon interaction associated with S-wave pion-nucleon scattering. The resulting contributions have been found to be very small in studies of the magnetic structure of the trinucleons [10].

The model-dependent currents are purely transverse and therefore cannot be directly linked to the underlying two-nucleon interaction. Among them, those associated with the Δ -isobar are the most important ones at moderate values of momentum-transfer ($q \leq 5 \text{ fm}^{-1}$). These currents are treated within the transition-correlation-operator scheme [10, 11], a scaled-down approach to a full $N+\Delta$ coupled-channel treatment. In this scheme, the Δ degrees of freedom are explicitly included in the nuclear wave functions by means of transition correlation operators that convert NN pairs into $N\Delta$ and $\Delta\Delta$ pairs, acting on a purely nucleonic wave function. Both $\gamma N\Delta$ and $\gamma\Delta\Delta$ M_1 couplings are considered with their values obtained from data [11].

The calculated isoscalar and isovector magnetic form factors of the trinucleons are shown in Fig. 2. The isovector form factor is underpredicted by theory in the first diffraction region. In this region, the π -like and ρ -like currents, constructed from the spin-spin and tensor components of the v_{18} interaction in the results shown in Fig. 2, is the dominant contribution, and therefore the underprediction mentioned above indicates that these currents are too weak at moderate values of momentum transfers. On the other hand, the isovector magnetic moment is in excellent agreement with the experimental value.

The isoscalar form factor appears to be slightly overpredicted by theory over the whole momentum transfer range. In particular, the calculated isoscalar magnetic moment is roughly 4 % too large with respect to the experimental value. This again points to

deficiencies in the model for two-body currents.

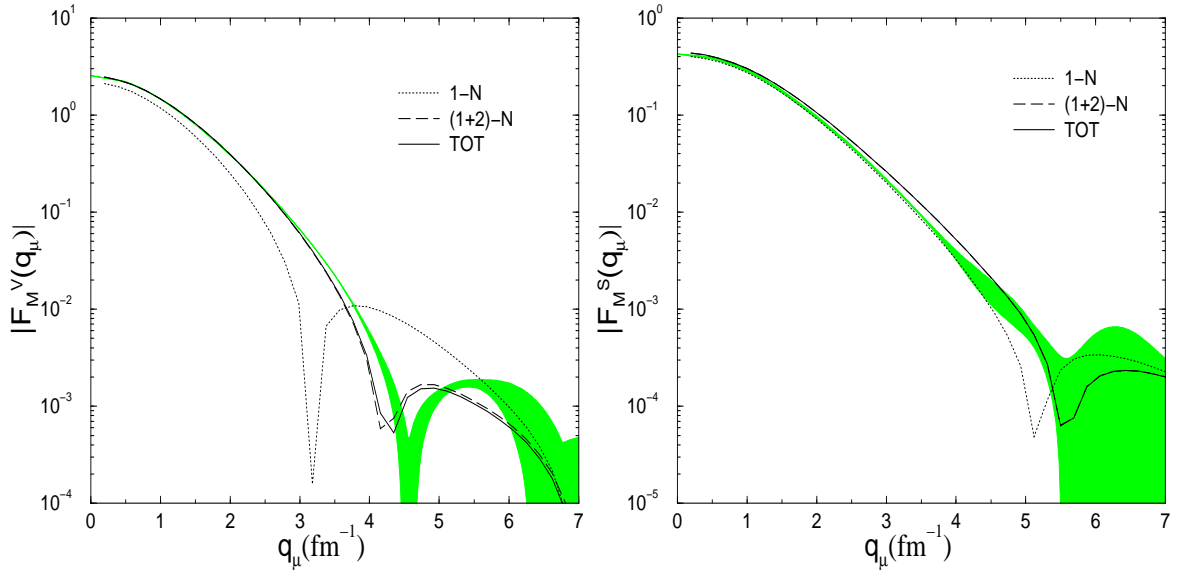


Figure 2. The isovector and isoscalar combinations of the ^3H and ^3He magnetic form factors obtained with the AV18/UIX Hamiltonian. The contributions associated with nucleonic one-body and (one+two)-body, and Δ currents are displayed.

While the model-independent two-body currents are linked to the form of nucleon-nucleon interaction via the continuity equation, the most important two-body charge operators are model dependent and may be viewed as relativistic corrections. They fall into two classes. The first class includes those effective operators that represent non-nucleonic degrees of freedom, such as nucleon-antinucleon pairs or nucleon-resonances, and which arise when these degrees of freedom are eliminated from the state vector. To the second class belong those dynamical exchange charge effects that would appear even in a description explicitly including non-nucleonic excitations in the state vector, such as the $\rho\pi\gamma$ transition coupling. The proper forms of the former operators depend on the method of eliminating the non-nucleonic degrees of freedom [4]. There are nevertheless rather clear indications for the relevance of two-body charge operators from the failure of calculations based on the one-body operator in predicting the charge form factors of the three- and four-nucleon systems, and deuteron tensor polarization observable.

The largest two-body charge contribution, at moderate values of the momentum transfer, is that due to the π -meson exchange operator. It is derived by considering the low-energy limit of the relativistic Born diagrams associated with the virtual π -meson photoproduction amplitude. In this limit, such an amplitude leads to two terms (at the lowest order). The first term consists of three factors: a single-nucleon charge operator, a non-relativistic propagator, and a OPE interaction. It is already included in the one-body (impulse approximation) calculation of the form factors, since the wave functions

used in these calculations are obtained from solutions of a Schrödinger equation including the OPE interaction. The second term, however, represents the truly two-body charge operator. It is a local operator with both isoscalar and isovector components. There are additional contributions due to the energy dependence of the pion propagator and direct coupling of the photon to the exchanged pion [4]. These operators, however, give rise to non-local isovector contributions which are expected to provide only small corrections to the leading local terms. For example these operators would only contribute to the isovector combination of the ^3He and ^3H charge form factors, which is anyway a factor of three smaller than the isoscalar. Thus they have been neglected in most of the studies I am familiar with.

The calculated ^3He and ^3H charge form factors are compared to data in Fig. 3. There is excellent agreement between theory and experiment. The important role of the two-body contributions above 3 fm^{-1} is also evident. The remarkable success of the present picture based on non-relativistic wave functions and a charge operator including the leading relativistic corrections should be stressed. It suggests, in particular, that the present model for the two-body charge operator is better than one *a priori* should expect. These operators fall into the class of relativistic corrections. Thus, evaluating their matrix elements with non-relativistic wave functions represents only the first approximation to a systematic reduction. A consistent treatment of these relativistic effects would require, for example, inclusion of the boost corrections on the nuclear wave functions. Yet, the excellent agreement between the calculated and measured charge form factors suggests that these corrections may be negligible in the q -range explored so far.

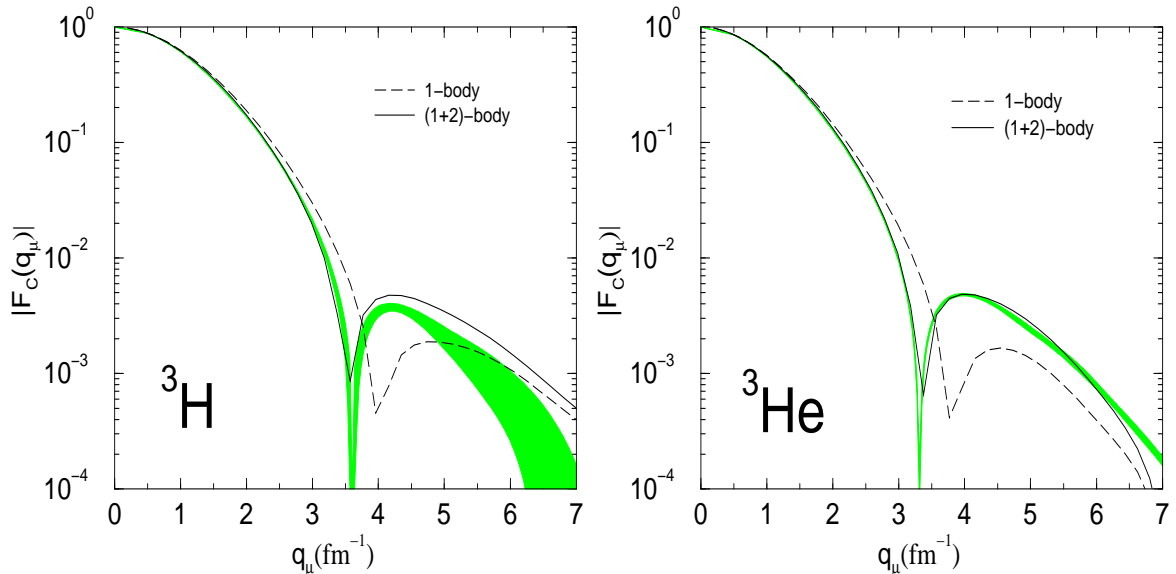


Figure 3. The ^3H and ^3He charge form factors obtained with the AV18/UIX Hamiltonian. The contributions associated with one-body and (one+two)-body operators are displayed.

4. Capture Reactions

4.1. The pd and nd Radiative Captures

There are now available many high-quality data, including differential cross sections, vector and tensor analyzing powers, and photon polarization coefficients, on the pd radiative capture at c.m. energies ranging from 0 to 2 MeV [12–15]. These data indicate that the reaction proceeds predominantly through S- and P-wave capture.

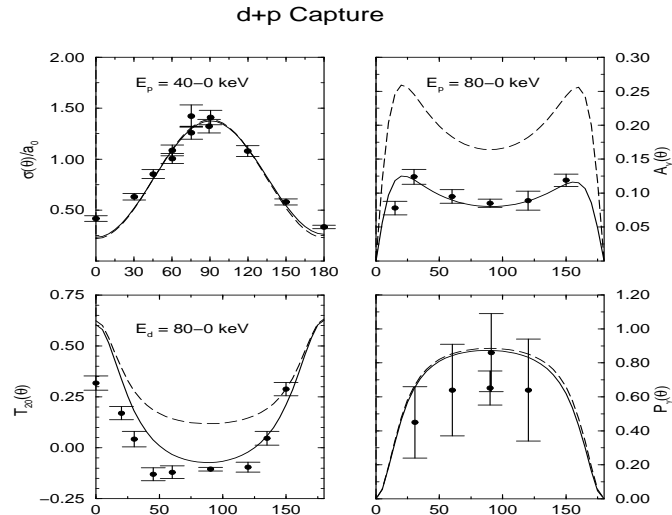


Figure 4. The energy integrated cross section $\sigma(\theta)/a_0$ ($4\pi a_0$ is the total cross section), vector analyzing power $A_y(\theta)$, tensor analyzing power $T_{20}(\theta)$ and photon linear polarization coefficient $P_\gamma(\theta)$ obtained with the AV18/UIX Hamiltonian model and one-body only (dashed line) or both one- and many-body (solid line) currents are compared with the experimental results of Ref. [12].

The predicted angular distributions [16] of the differential cross section $\sigma(\theta)$, vector and tensor analyzing powers $A_y(\theta)$ and $T_{20}(\theta)$, and photon linear polarization coefficient $P_\gamma(\theta)$ are compared with the TUNL data below 50 keV from Refs. [12,14] in Fig 4. Note that the AV18/UIX Hamiltonian model is used in the calculations reported here. The agreement between the full theory, including many-body current contributions, and experiment is generally good. However, a closer inspection of the figure reveals the presence of significative discrepancies between theory and experiment in the small angle behavior of $\sigma(\theta)$ and $T_{20}(\theta)$, as well as in the S -factor below 40 keV [16]. The S-wave capture proceeds mostly through the M_1 transitions connecting the doublet and quartet pd states to ${}^3\text{He}$ —the associated reduced matrix elements (RMEs) are denoted by m_2 and m_4 , respectively. The situation for P-wave capture is more complex, although at energies below 50 keV it is dominated by the E_1 transitions from the doublet and quartet pd states having channel spin $S=1/2$, whose RMEs I denote as p_2 and p_4 . The E_1 transitions involving the channel spin $S = 3/2$ states, while smaller, do play an important role in $T_{20}(\theta)$.

The TUNL [14] and Wisconsin [15] groups have determined the leading M_1 and E_1

RMEs via fits to the measured observables. The results of this fitting procedure are compared with the calculated RMEs in Table 1. The phase of each RME is simply related to the elastic pd phase shift [15], which at these low energies is essentially the Coulomb phase shift. As can be seen from Table 1, the most significant differences between theoretical and experimental RMEs are found for $|p_4|$. The theoretical overprediction of p_4 is the cause of the discrepancies mentioned above in the low-energy (≤ 50 keV) S -factor and small angle $\sigma(\theta)$.

It is interesting to analyze the ratio $r_{E1} \equiv |p_4/p_2|^2$. Theory gives $r_{E1} \simeq 1$, while from the fit it results that $r_{E1} \approx 0.74 \pm 0.04$. It is important to stress that the calculation of these RMEs is not influenced by uncertainties in the two-body currents, since their values are entirely given by the long-wavelength form of the E_1 operator (Siegert's theorem), which has no spin-dependence (for a thorough discussion of the validity of the long-wavelength approximation in E_1 transitions, particularly suppressed ones, see Ref. [16]). It is therefore of interest to examine more closely the origin of the above discrepancy. If the interactions between the p and d clusters are switched off, the relation $r_{E1} \simeq 1$ then simply follows from angular momentum algebra. Deviations of this ratio from one are therefore to be ascribed to differences induced by the interactions in the $S=1/2$ doublet and quartet wave functions. The interactions in these channels do not change the ratio above significantly. It should be emphasized that the studies carried out up until now ignore, in the continuum states, the effects arising from electromagnetic interactions beyond the static Coulomb interaction between protons. It is not clear whether the inclusion of these long-range interactions, in particular their spin-orbit component, could explain the splitting between the p_2 and p_4 RMEs observed at very low energy. This discrepancy seems to disappear at 2 MeV [16].

Table 1

Magnitudes of the leading M_1 and E_1 RMEs for pd capture at $E_p = 40$ keV.

RME	IA	FULL	FIT
$ m_2 $	0.172	0.322	0.340 ± 0.010
$ m_4 $	0.174	0.157	0.157 ± 0.007
$ p_2 $	0.346	0.371	0.363 ± 0.014
$ p_4 $	0.343	0.378	0.312 ± 0.009

Finally, the doublet m_2 RME is underpredicted by theory at the 5 % level. On the other hand, the cross section for nd capture at thermal neutron energy is calculated to be $229 \mu\text{b}$ with one-body currents and $578 \mu\text{b}$ with one- and many-body currents, using the AV18/UIX Hamiltonian model [18]. This last result is 15 % larger than the experimental value $(508 \pm 15) \mu\text{b}$ [17]. Of course, M_1 transitions (which induce the nd capture), particularly doublet ones, are significantly influenced by many-body current contributions. This is an unsettling state of affairs: on the one hand, theory underpredicts the doublet M_1 “experimental” RME for pd capture (see Table 1), while overpredicting, on the other hand, the nd capture cross section, which is dominated by the doublet M_1 transition.

4.2. The αd Radiative Capture

Radiative capture of deuterons on α particles is the only process by which ${}^6\text{Li}$ is produced in standard primordial nucleosynthesis models [19]. There are no direct αd capture data in the energy region relevant for big bang nucleosynthesis (BBN), and it is therefore crucial to have a reliable theoretical estimate for the $d(\alpha, \gamma){}^6\text{Li}$ cross section.

In fact, the theoretical description of the αd capture is particularly challenging: the S- and P-wave captures are strongly inhibited by quasi-orthogonality between the initial and final states and by an isospin selection rule, respectively. As a result, the dominant process in all experiments performed to date has been electric quadrupole (E_2) capture from D-wave scattering states. The small remaining E_1 contribution from P-wave initial states has been observed at about 2 MeV, but its magnitude has not been successfully explained by theoretical treatments; it is generally expected to contribute half of the cross section at 100 keV. The S-wave capture induced by M_1 has been neglected in most calculations because of the quasi-orthogonality mentioned above, which makes the associated matrix element identically zero in two-body treatments of the process. The energy dependences of the various capture mechanisms (E_2 , E_1 , M_1) are such that even E_1 and M_1 captures with small amplitudes may become important at low (< 200 keV) energies. Low-energy behavior is particularly important for standard BBN: the primordial ${}^6\text{Li}$ yield is only sensitive to the capture cross section between 20 and 200 keV, with the strongest sensitivity at 60 keV [20].

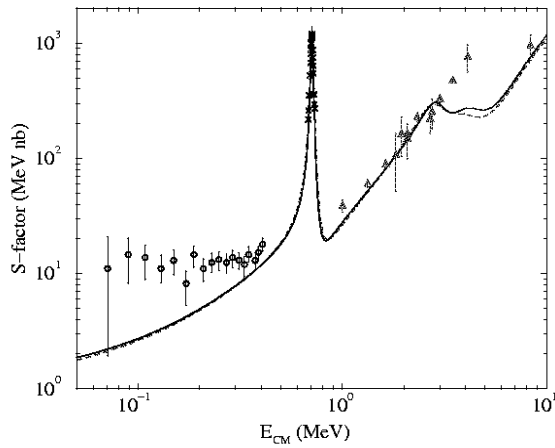


Figure 5. The calculated αd S-factor, as obtained from two distinct αd potentials (see text), is compared to available data.

Recently, a calculation of the αd capture has been carried out [21] using variational Monte Carlo wave functions to describe the initial αd S-, P-, and D-wave scattering

states and final ${}^6\text{Li}$ bound-state, and including M_1 , E_1 , and E_2 transitions. The resulting S -factor is compared with available data in Fig. 5. While this calculation is not in the same league as the three-body capture calculations discussed in the previous section or the $p\,{}^3\text{He}$ weak capture calculation presented by Marcucci in these proceedings [22], it is, nevertheless, the first attempt to a microscopic description of a six-body capture process. At present, the αd relative wave function is obtained from a phenomenological potential, fitted to αd elastic scattering data, and the ${}^6\text{Li}$ variational wave function gives an energy that is higher than that corresponding to separated α and d clusters. These aspects of the calculation are clearly unsatisfactory. For example, the orthogonality between the αd S -wave scattering state and ${}^6\text{Li}$ bound state needs to be enforced artificially. Some of these limitations can be easily overcome, for example one could use a Green's function Monte Carlo wave function for ${}^6\text{Li}$, which does reproduce the experimental binding energy. Others, however, are more challenging, one clearly belonging to this class is the calculation of the αd scattering state from the six-body realistic Hamiltonian. This is perhaps the central problem in calculations of capture processes involving systems with $A > 4$.

5. Acknowledgments

I wish to thank J. Carlson, J.L. Forest, A. Kievsky, L.E. Marcucci, K.M. Nollett, V.R. Pandharipande, S.C. Pieper, D.O. Riska, S. Rosati, M. Viviani, and R.B. Wiringa for their many important contributions to the work reported here. This work was supported by DOE contract DE-AC05-84ER40150 under which the Southeastern Universities Research Association (SURA) operates the Thomas Jefferson National Accelerator Facility.

REFERENCES

1. R. Machleidt, F. Sammarruca, and Y. Song, Phys. Rev. C **53**, R1483 (1996); R. Machleidt, nucl-th/0006014.
2. R.B. Wiringa, V.G.J. Stoks, and R. Schiavilla, Phys. Rev. C **51**, 38 (1995).
3. J.R. Bergervoet *et al.*, Phys. Rev. C **41**, 1435 (1990); V.G.J. Stoks, R.A.M. Klomp, M.C.M. Rentmeester, and J.J. de Swart, Phys. Rev. C **48**, 792 (1993).
4. J.L. Friar, Ann. Phys. (N.Y.) **104**, 380 (1977); S.A. Coon and J.L. Friar, Phys. Rev. C **34**, 1060 (1986).
5. R.B. Wiringa, S.C. Pieper, J. Carlson, and V.R. Pandharipande, Phys. Rev. C **62**, 014001 (2000).
6. A. Nogga, H. Kamada, and W. Glöckle, Phys. Rev. Lett. **85**, 944 (2000).
7. J. Carlson, these proceedings.
8. J. Fujita and H. Miyazawa, Prog. Theor. Phys. **17**, 360 (1957).
9. J. Carlson and R. Schiavilla, Rev. Mod. Phys. **70**, 743 (1998).
10. L.E. Marcucci, D.O. Riska, and R. Schiavilla, Phys. Rev. C **58**, 3069 (1998).
11. R. Schiavilla, R.B. Wiringa, V.R. Pandharipande, and J. Carlson, Phys. Rev. C **45**, 2628 (1992).
12. G.J. Schmid *et al.*, Phys. Rev. Lett. **76**, 3088 (1996).
13. L. Ma *et al.*, Phys. Rev. C **55**, 588 (1997).
14. E.A. Wulf *et al.*, Phys. Rev. C **61**, 021601(R) (1999).
15. M.K. Smith and L.D. Knutson, Phys. Rev. Lett. **82**, 4591 (1999).

16. M. Viviani, A. Kievsky, L.E. Marcucci, S. Rosati, and R. Schiavilla, Phys. Rev. C **61**, 064001 (2000).
17. E.T. Journey, P.J. Bendt, and J.C. Browne, Phys. Rev. C **25**, 2810 (1982).
18. M. Viviani, R. Schiavilla, and A. Kievsky, Phys. Rev. C **54**, 534 (1996).
19. K.M. Nollett, M. Lemoine, and D.N. Schramm, Phys. Rev. C **56**, 1144 (1997).
20. K.M. Nollett and S. Burles, Phys. Rev. D **62**, 123505 (1999).
21. K.M. Nollett, R.B. Wiringa, and R. Schiavilla, nucl-th/0006064, Phys. Rev. C in press.
22. L.E. Marcucci, these proceedings.